Inorg. Chem. **2005**, *44*, 1626–1634

Synthesis, Characterization, and Electrochemistry of Biorelevant Photosensitive Low-Potential Orthometalated Ruthenium Complexes

Alexander D. Ryabov,*,† Ronan Le Lagadec,‡ Hebert Estevez,‡ Ruben A. Toscano,‡ Simon Hernandez,‡ Larissa Alexandrova,§ Viktoria S. Kurova,|| Andreas Fischer,⊥ Claude Sirlin,# and Michel Pfeffer#

Department of Chemistry, Carnegie Mellon University, 4400 Fifth Avenue, Pittsburgh, Pennsylvania 15213, Instituto de Química, UNAM, Circuito Exterior s/n, Ciudad Universitaria, Mexico, D. F., 04510, Mexico, Instituto de Investigaciones en Materiales, UNAM, Circuito Exterior s/n, Ciudad Universitaria, Mexico, D. F., 04510, Mexico, Department of Chemistry, Moscow State University, 119899, Moscow, Russia, Inorganic Chemistry, Department of Chemistry, Royal Institute of Technology, S-100 44 Stockholm, Sweden, and Laboratoire de Synthèses Métallo-Induites, UMR CNRS 7513 Université Louis Pasteur 4, rue Blaise Pascal 67070 Strasbourg, France

Received December 9, 2004

Redox potentials of photosensitive cyclometalated Ru^{II} derivatives of 2-phenylpyridine or 2-(4-tolyl)pyridine are controllably decreased by up to 0.8 V within several minutes. This is achieved by irradiation of the ruthena(II)cycles *cis*-[Ru(*o*-X-2-py)(LL)$(MeCN)_2$]PF_6 (**2**, X = C_6H_4 (**a**) or 4-MeC_6H_3 (**b**), LL = 1,10-phenanthroline or 2,2′-bipyridine). The cis geometry of the MeCN ligands has been confirmed by the X-ray structural studies. The σ-bound sp^2 carbon of the metalated ring is trans to LL nitrogen. Complexes **2** are made from [Ru(*o*-X-2-py)$(MeCN)_4$]PF_6 (**1**) and LL. This "trivial" ligand substitution is unusual because **1a** reacts readily with phen in MeCN as solvent to give *cis*-[Ru(*o*-C_6H_4-2-py)(phen)$(MeCN)_2$]PF_6 (**2c**) in a 83% yield, but bpy does not afford the bpy-containing **2** under the same conditions. *cis*-[Ru(*o*-C_6H_4-2-py)(bpy)$(MeCN)_2$]PF_6 (**2e**) has been prepared in CH_2Cl_2 (74%). Studies of complexes **2c**,**e** by cyclic voltammetry in MeOH in the dark reveal $Ru^{II/III}$ quasy-reversible redox features at 573 and 578 mV (vs Ag/AgCl), respectively. A minute irradiation **2c** and **2e** converts them into new species with redox potentials of −230 and 270 mV, respectively. An exceptional potential drop for **2c** is accounted for in terms of a photosubstitution of both MeCN ligands by methanol. ESR, ^1H NMR, and UV–vis data indicate that the primary product of photolysis of **2c** is an octahedral monomeric low-spin ($S = {}^1/_2$) Ru^{III} species, presumably *cis*-[Ru^{III}(*o*-C_6H_4-2-py)(phen)$(MeOH)_2$]$^{2+}$. The primary photoproduct of bpy complex **2e** is *cis*-[Ru^{II}(*o*-C_6H_4-2-py)(bpy)(MeCN)(MeOH)]$^+$, and this accounts for a lower decrease in the redox potential. Irradiation of **2c** in the presence of added chloride affords [(phen)(*o*-C_6H_4-2-py)ClRu^{III}ORu^{IV}Cl(*o*-C_6H_4-2-py)(phen)]PF_6, a first μ-oxo-bridged mixed valent dimer with a cyclometalated unit. The structure of the dimer has been established by X-ray crystallography.

Introduction

Materials capable of rapid and dramatic variation of physicochemical characteristics on exposure to light, changes in pressure, temperature, acidity, humidity, etc., are in a strong demand by modern sensor and electronic nanotechnology.[1−3] In bioelectronics,[4] such materials are used as components of bioamperometric analytical devices,[5,6] if a low molecular weight compound, the redox potential of which is adjustable by irradiation, moves fast electrons between the active sites of redox enzymes and an electrode.[7,8] These molecules are referred to as electron shuttles or mediators,

* Author to whom correspondence should be addressed. E-mail: ryabov@andrew.cmu.edu.
† Carnegie Mellon University.
‡ Instituto de Química, Ciudad Universitaria.
§ Instituto de Investigaciones en Materiales, Ciudad Universitaria.
|| Moscow State University.
⊥ Royal Institute of Technology.
Université Louis Pasteur.

(1) Bissell, R. A.; Cordova, E.; Kaifer, A. E.; Stoddart, J. F. *Nature (London)* **1994**, *369*, 133−137.
(2) Zhang, S. *Biotechnol. Adv.* **2002**, *20*, 321−339.
(3) von Molnar, S.; Read, D. *Physica B* **2002**, *318*, 113−118.
(4) Willner, I.; Willner, B. *Trends Biotechnol.* **1001**, *19*, 222−230.
(5) Willner, I.; Willner, B. *Bioelectrochem. Bioenerg.* **1997**, *42*, 43−57.
(6) Willner, I.; Katz, E. *Angew. Chem., Int. Ed.* **2000**, *39*, 1180−1218.

10.1021/ic048270w CCC: $30.25
Published on Web 02/10/2005

Chart 1. Principal Compounds Used in This Study[a]

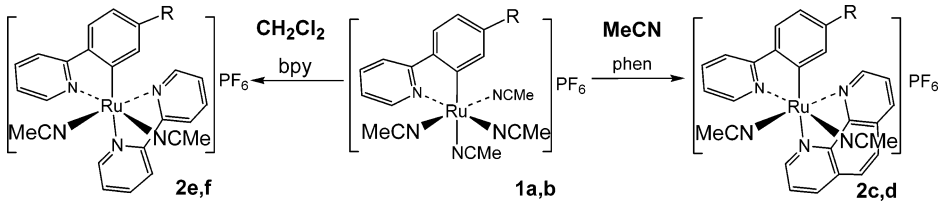

[a] R = H (**a**, **c**, **e**) and Me (**b**, **d**, **f**).

and many of them are transition metal complexes.[9] In a series of previous papers, we have introduced cyclometalated ruthenium(II)[10−13] and osmium(II)[14] complexes as superb mediators of several oxidoreductases. The redox potentials of ruthenacycles $[Ru(o\text{-}C_6H_4\text{-}Z)(LL)(LL')]PF_6$ (Z = 2-pyridinyl, 2-imidazolyl, CH_2NMe_2; LL/LL′ = bpy, phen) are in the 150−400 mV range, and the ruthenacycles exchange electrons fast with glucose oxidase (GO),[10,11] PQQ-dependent glucose dehydrogenase (PQQ = pyrroloquinoline quinone),[13] or peroxidazes from horseradish (HRP), sweet potato, and royal palm tree.[10,12] The rate constants for the reduction of oxidized states of peroxidases by Ru^{II} reach the level of 10^8 M^{-1} s^{-1}. The rate constants for the oxidation of reduced GO and PQQ-dependent glucose dehydrogenase by the corresponding Ru^{III} species are around 10^6-10^7 M^{-1} s^{-1}. Structurally analogous cyclometalated osmium complexes are as reactive as their ruthenium counterparts but more advantageous as mediators of GO due to significantly lower redox potentials, which can be as low as −100 mV.[14] The cyclometalated Ru^{II} and Os^{II} complexes are resistant to substitution. Their redox potentials are therefore not subjected to quick variation. A goal of this work has been syntheses and studies of enzymically relevant, structurally related cyclometalated Ru^{II} derivatives with photolabile π-acceptor N-donor ligands, the redox potentials of which could rapidly and controllably be lowered by light. A photoinduced solvolytic substitution of the π-acceptor ligands (in solvents such as water, methanol, acetone, etc.) by ligands, the electrochemical Lever parameters E_L of which are lower than those of the leaving groups,[15] should have generated in situ species with notably lower redox potentials. The potentials of cyclometalated Ru^{II} complexes reported here are adjustable to a lower level typical of the corresponding osma(II)cycles (usually by ∼300 mV lower than of their Ru^{II} counterparts). In particular, we describe new synthetic, structural, and photodynamic chemistry of cyclometalated Ru^{II} complexes of 2-phenylpyridine and 2-(4-tolyl)pyridine with cis acetonitrile ligands (**2** in Chart 1). The redox potentials of the **2** ruthenacycles are controllably reduced by 0.3−0.8 V in minutes by irradiation with visible light. A curious example is described with bidentate N-donor ligands as 1,10-phenanthroline is indeed able to readily substitute two cis MeCN ligands at Ru^{II}, whereas 2,2′-bipyridine cannot be coordinated to the Ru^{II} center under similar conditions.

Results and Discussion

Basic Synthetic Procedures. Starting complexes **1a**,**b** have been synthesized by cycloruthenation of the parent amines, 2-phenylpyridine (C_6H_5-2-py) and 2-(4-tolyl)pyridine (MeC_6H_4-2-py), by $[(\eta^6\text{-}C_6H_6)RuCl(\mu\text{-}Cl)]_2$.[16] Lemon-yellow solid complex **1a** is unstable in the air and turns gradually yellowish green and then dark green.[16] This, however, does not affect its further reactions, and numerous cyclometalated derivatives of the type $[Ru(o\text{-}C_6H_4\text{-}2\text{-py})(LL)_2]PF_6$ (LL = bpy or phen) have been prepared in MeOH as solvent.[10] We anticipated thus that performing this reaction with a 1:1 stoichiometry between **1a** and phen or bipy should afford complexes such as $[Ru(o\text{-}C_6H_4\text{-}2\text{-py})(LL)(MeCN)_2]PF_6$, that is, in which the bidentate LL ligand has substituted two MeCN ligands in **1a**. This worked indeed readily with 1,10-phenanthroline as the bidentate ligand, and complex **2c** was isolated in a good yield. However, similar reactions of complexes **1a** and **1b** did not work for py and bpy under identical conditions.[17] Such different behavior of closely related ligands could tentatively be rationalized in terms of a principally dissociative mechanism of the ligand substitution at Ru^{II} shown in Scheme 1.[18,19] In general, the rates of ligand replacement at Ru^{II} are higher for substituted pyridines with higher pK_a values.[20] However, the most basic ligand in the series used here, that is, pyridine (pK_a's of py, bpy, and phen equal 5.24, 4.4, and 4.9, respectively[21]), does not replace MeCN in **1a**, suggesting that the overall substitution is thermodynamically controlled. The fact that MeCN is 3 times as reactive as pyridine with respect to Ru^{II} found by Allen

(7) Turner, A. P. F.; Karube, I.; Wilson, G. S. *Biosensors. Fundamentals and Applications*; Oxford University Press: Oxford, New York, Tokyo, 1987.
(8) Dequaire, M.; Limoges, B.; Moiroux, J.; Saveant, J.-M. *J. Am. Chem. Soc.* **2002**, *124*, 240−253.
(9) Ryabov, A. D. *Adv. Inorg. Chem.* **2004**, *55*, 201−270.
(10) Ryabov, A. D.; Sukharev, V. S.; Alexandrova, L.; Le Lagadec, R.; Pfeffer, M. *Inorg. Chem.* **2001**, *30*, 6529−6532.
(11) Soukharev, V. S.; Ryabov, A. D.; Csöregi, E. *J. Organomet. Chem.* **2003**, *668*, 75−81.
(12) Alpeeva, I. S.; Soukharev, V. S.; Alexandrova, L.; Shilova, N. V.; Bovin, N. V.; Csöregi, E.; Ryabov, A. D.; Sakharov, I. Y. *J. Biol. Inorg. Chem.* **2003**, *8*, 683−688.
(13) Le Lagadec, R.; Rubio, L.; Alexandrova, L.; Toscano, R. A.; Ivanova, E. V.; Meškys, R.; Laurinavicius, V.; Pfeffer, M.; Ryabov, A. D. *J. Organomet. Chem.* **2004**, *689*, 4820−4832.
(14) Ryabov, A. D.; Soukharev, V. S.; Alexandrova, L.; Le Lagadec, R.; Pfeffer, M. *Inorg. Chem.* **2003**, *42*, 6598−6600.
(15) Lever, A. B. V. *Inorg. Chem.* **1990**, *29*, 1271−1285.
(16) Fernandez, S.; Pfeffer, M.; Ritleng, V.; Sirlin, C. *Organometallics* **1999**, *18*, 2390−2394.
(17) When bpy reacts with **1a** or **1b** in MeCN under identical conditions, the solutions turn brown. New brownish-orange crystalline materials have been isolated in both cases. The composition of both products appears to be identical to that of **1a** and **1b**. These facts are currently under intensive investigation.
(18) Wilkins, R. G. *Kinetics and Mechanism of Reactions of Transition Metal Complexes*, 2nd ed.; VCH: Weinheim, 1991.
(19) Burgess, J.; Hubbard, C. D. *Adv. Inorg. Chem.* **2003**, *54*, 72−155.
(20) Allen, R. J.; Ford, P. C. *Inorg. Chem.* **1972**, *11*, 679−685.
(21) Smith, R. M.; Martell, A. E. *Critical Stability Constants, Vol. 2: Amines*; Plenum Press: New York and London, 1975.

Scheme 1. Plausible Dissociative Mechanisms for the Formation of Complexes **2**

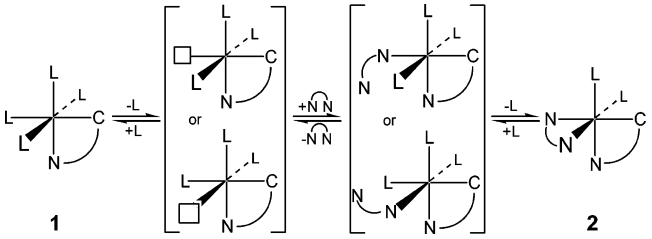

and Ford[20] supports this assumption. It is thus understood why pyridine does not substitute coordinated MeCN in acetonitrile as solvent. The inability of bpy, in contrast to phen, to react with **1** to give **2** in MeCN is likely due to the fact that the stability of phen complexes is by the order of magnitude higher than that of the corresponding bpy complexes. An assumption made is that the trend holds for Ru^{II} as it does for related Fe^{II} species.[21]

The Ru−N bond in a trans position relative to the σ-bound carbon is the longest in **1a** (2.154 Å), indicative of its ground-state destabilization. This Ru−N bond should be dissociatively cleaved first. The position of the phen nitrogen trans to the metalated carbon in complexes **2c** and **2d** has been proved by the X-ray crystallography (see below). Dissociation of one of the two acetonitriles in a trans position cannot also be excluded. The intermediates shown in Scheme 1 could exist in reactions with py and bpy, but the products of ligand substitution **2** are not isolated as solids because of their lower thermodynamic stability as compared to **1a**.

Several efforts were made to synthesize complexes of type **2** with coordinated 2,2′-bipyridine. The complex $[Ru(o\text{-}C_6H_4\text{-}2\text{-}py)(bpy)_2]PF_6$ was obtained from **1a** and bpy in refluxing methanol.[10] When the same procedure was applied using bpy in deficiency with respect to **1a**, the target complex **2e** was not detected and $[Ru(o\text{-}C_6H_4\text{-}2\text{-}py)(bpy)_2]PF_6$ was isolated instead. A mixture of $[Ru(o\text{-}C_6H_4\text{-}2\text{-}py)(bpy)_2]PF_6$ and **2e** was obtained when the reaction was carried out in CH_2Cl_2 at ambient temperature using 0.9 equiv of bpy. Complex **2e** was isolated in a 74% yield by using column chromatography (Al_2O_3/CH_2Cl_2).

X-ray Structural Characterization of Complexes 1a, 1b, 2c, and 2e. X-ray crystal structures of complexes **1a** and **1b** are shown in Figure 1. An octahedral polyhedron around Ru^{II} in complexes **1** consists of one σ-bound sp^2 carbon, four acetonitrile, and one pyridine nitrogens. The Ru−N bond lengths are similar for all nitrogens, but the bond located in a trans position with respect to the σ-bound carbon is longer due to the ground-state destabilization, as expected. Both complexes **1** crystallize as diethyl ether solvates. The Ru:Et_2O ratio equals 1 and 0.5 in **1a** and **1b**, respectively. A localization of the ether deserves a comment. In **1a**, the molecule of diethyl ether lies almost in the plane of the cyclometalated 2-phenylpyridine ligand. There is a rather short O1···C5 contact of 3.688 Å (the corresponding O1···H−C5 separation equals 2.795 Å). The "in-plane" geometry is stabilized by the C13···C21 contact (4.185 Å) involving methyl groups of the ether and the "in-plane" coordinated acetonitrile. A shielding of the key carbon by a methyl group in the 2-(4-tolyl)pyridine complex **1b** changes the position of the ether. The shortest contact of 4.19 Å is observed between O1 and C10. Diethyl ether is below the plane of the cyclometalated ligand; stabilization through the C23a···C15 contact (4.498 Å) is likely.

Among bis acetonitrile complexes **2**, the X-ray structural characterization has been performed for ruthenacycles **2c** and **2d**. The structure of **2d** is shown in Figure 2. The structure of **2c** (Figure 1S) has been solved with a lower accuracy, but its geometrical identity with **2d** is obvious. General features of complexes **2** include (i) a cis configuration of the MeCN ligands and (ii) the fact that one of the phen nitrogens is located trans to the σ-bound carbon of the cyclometalated ligand. The corresponding Ru−N bond length is longer as compared to the Ru−N bond of phen, which is in a trans position with respect to MeCN. More careful inspection of bond lengths of complex **2d** indicates that the Ru−N_{phen} bond distances are longer as compared to the Ru−N_{MeCN} distances due to a more pronounced back-bonding capability of coordinated acetonitrile as compared to phen. A similar trend is typical of complexes **1b** and **2e**. The Ru−C bond is slightly longer in **1b** when acetonitrile is coordinated in a trans position. Correspondingly, the Ru−N4 bond length of **1b** is the longest (2.162 Å), manifesting a strong σ-donor effect from the tolyl carbon. The σ-donor effect disfavors an electron flow from the MeCN ligand to the metal, and the corresponding Ru−N bond becomes longer. This Ru−N bond length (trans to carbon) in complex **1a** equals 2.153 Å.

Phototunable Electrochemistry of Complexes 2. Cyclic voltammograms of complexes **2** obtained at a glassy carbon working electrode in acetonitrile and methanol in the potential range from −1 to +1 V versus Ag/AgCl in the absence of irradiation are characterized by a single quasi-reversible $Ru^{II/III}$ redox feature around 0.5 V (Table 1). The electrochemical properties of the intact ruthenancycles **2** and complexes $[Ru(o\text{-}C_6H_4\text{-}2\text{-}py)(LL)_2]PF_6$ reported previously[10] are similar. The redox potentials of complexes **2** are somewhat shifted anodically as compared to the corresponding species $[Ru(o\text{-}C_6H_4\text{-}2\text{-}py)(LL)_2]PF_6$, reflecting the fact that the E_L values for MeCN are slightly higher than for both phen and bpy, 0.34 versus 0.26 and 0.259, respectively.[15] A stronger back-bonding capability of acetonitrile ligands as compared to phen and bpy is manifested here as well. Cyclic voltammograms of $[Ru(o\text{-}C_6H_4\text{-}2\text{-}py)(phen)_2]PF_6$ obtained in MeOH as solvent do not change on irradiation. Structurally related phen-containing complex **2c** behaves differently under the same conditions. Its cyclic voltammograms change dramatically in minutes when the solution is irradiated by visible light (Figure 3). There is a single well-defined redox feature at 0.57 V before irradiation (Figure 3a), which disappears rapidly in the presence of light. A new major redox wave evolves simultaneously at −0.23 V, and the initial wave is practically gone after irradiation for 7 min (Figure 3b). An overall potential drop is exceptional and is as high as 0.8 V! It is convenient to monitor the peak current at 0.63 V, and the inset in Figure 3 illustrates its exponential decrease. The calculated conditional pseudo-first-order rate

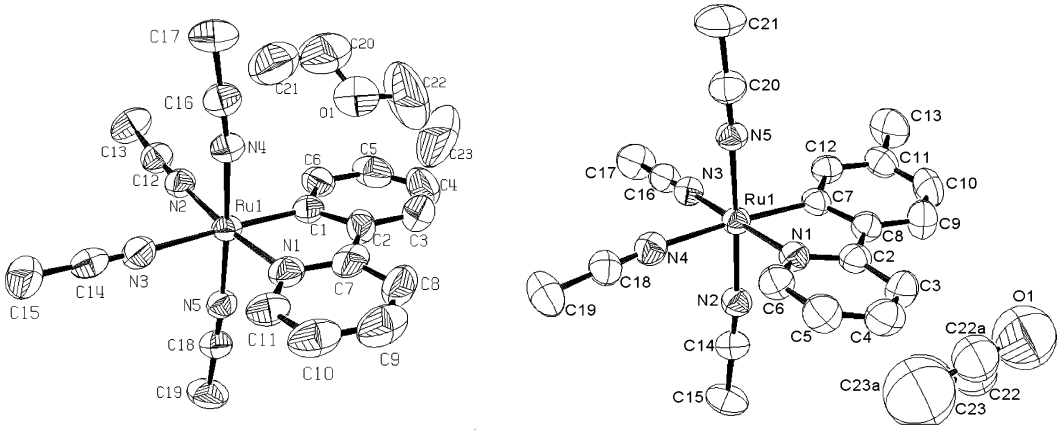

Figure 1. ORTEP diagrams for cationic complexes **1a** and **1b** (H atoms and the PF_6^- counterion are not shown for clarity). Ellipsoids represent a 50% probability level. Selected bond lengths for **1a**: Ru−C1 2.014(6), Ru−N1 2.051(5), Ru−N2 2.055(6), Ru−N3 2.154(6), Ru−N4 2.019(5), and Ru−N5 2.015(5) Å. Selected bond lengths for **1b**: Ru−C7 2.024(5), Ru−N1 2.009(4), Ru−N2 2.021(4), Ru−N3 2.034(4), Ru−N4 2.162(6), and Ru−N5 2.009(4) Å.

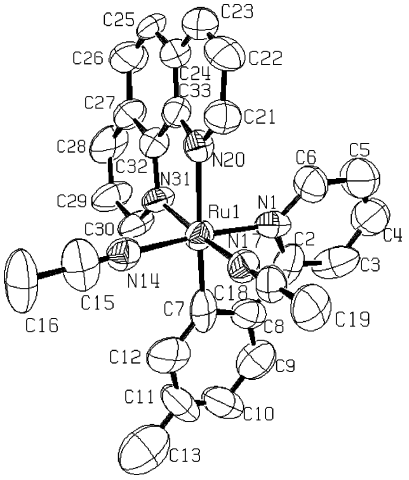

Figure 2. ORTEP diagram for the cationic part of complex **2d**. Ellipsoids represent a 50% probability level. Selected bond lengths: Ru−N14 1.989(5), Ru−N1 1.996(5), Ru−C7 1.997(8), Ru−N17 2.002(4), Ru−N31 2.047(4), Ru−N20 2.137(4) Å.

constant k_{obs} equals $(6.2 \pm 0.4) \times 10^{-3}$ s^{-1}, and this corresponds to the half-life ($\tau_{1/2}$) of 1.86 min. Electron richer complex **2d** with analogous diimine phen ligand behaves identical to **2c**. The corresponding electrochemical data are shown in Table 1; k_{obs} equals $(5.9 \pm 1.9) \times 10^{-3}$ s^{-1} and $\tau_{1/2} = 1.95$ min.

The changes shown in Figure 3 for complex **2c** could be understood assuming that the primary process is a photochemical solvolysis of MeCN ligands as shown in Scheme 2. In fact, if both MeCN ligands are substituted by MeOH to afford **2″**, the corresponding potential shift could be estimated using the E_L values for the ligands involved.[15] Because E_L for MeOH is not reported, it may be approximated by the value for water (0.04), which is perhaps slightly higher than E_L for MeOH because of an electron-donating effect from the methyl group. Because $E_L = 0.34$ for MeCN, the expected potential drop should not be less than 0.6 V $((0.34 \times 2) - (0.04 \times 2))$, and this agrees satisfactorily with the experimental 0.8 V. A poorly defined electrochemical feature seen around 0.25 V (Figure 3b) could be rationalized by assuming an intermediate formation of **2′** with one acetonitrile ligand being substituted by the solvent. Interestingly, the monosubstitution dominates for the 2,2′-bipyridine complexes **2e**,**f**. The results of electrochemical monitoring of early stages of photosolvolysis of **2f** in MeOH are demonstrated in Figure 4.

The disappearance of the starting material observed at 0.58 V is accompanied by a generation of a new species at 0.27 V. The potential drop equals 0.3 V and agrees with the substitution of a single MeCN ligand and the formation of **2e′**. The solvolysis of complex **2e** occurs slower than that of **2c**. In this case, it is more convenient to follow a peak current increase at 0.31 V, and the corresponding exponential growth is shown as the inset to Figure 4. The calculated conditional k_{obs} value equals $(2.31 \pm 0.08) \times 10^{-3}$ s^{-1} and $\tau_{1/2} = 5$ min. Substitution of the second ligand becomes noticeable after 20 min, and the overall conversion of **2e** into **2e″** is incomplete even after 35 min. The behavior of complex **2f** is practically the same as that of **2e**. Its electrochemical characteristics are in Table 1; k_{obs} equals $(2.9 \pm 0.1) \times 10^{-3}$ s^{-1} and $\tau_{1/2} = 4$ min. Thus, the photodynamic performance of structurally similar complexes **2** with bidentate diimine phen or bpy ligands differs in two aspects. First, the photosolvolysis of **2-phen** species occurs at least twice as fast as that of **2-bpy**, and, more importantly, the species with significantly different redox potentials are produced (−0.23 and 0.27 V in the case of **2c** and **2e**, respectively). This suggests a versatile technique for in situ photochemical generation of the species with a desired redox potential; photolysis of the bpy or phen complexes will adjust fine or coarse tuning, respectively.

Although it has been known that the substitution of MeCN and py by other ligands at Ru^{II} is facilitated by light,[22−25]

(22) Ford, P. C.; Petersen, J. D.; Hintze, R. E. *Coord. Chem. Rev.* **1974**, *14*, 67−105.
(23) Durham, B.; Walsh, J. L.; Carter, C. L.; Meyer, T. J. *Inorg. Chem.* **1980**, *19*, 860−865.
(24) Laemmel, A.-C.; Collin, J.-P.; Sauvage, J.-P. *C. R. Acad. Sci., Ser. Iic: Chim.* **2000**, *3*, 43−49.
(25) Schofield, E. R.; Collin, J.-P.; Gruber, N.; Sauvage, J.-P. *J. Chem. Soc., Chem. Commun.* **2003**, 188−189.

Table 1. Electrochemical, Spectral Properties of Intact and Irradiated Complexes **2** in MeCN and MeOH, and Estimated Half-lives ($\tau_{1/2}$) for the Photochemical Transformations of Complexes **2** at Room Temperature (Potentials vs Ag/AgCl; Data for [Ru(*o*-C_6H_4-2-py)(phen)$_2$]PF_6 Are Included for Comparison)

complex **2** (R/N^N)	$E_{1/2}$/mV in MeCN (0.1 M $^nBu_4NPF_6$)	$E_{1/2}$/mV in MeOH (0.1 M $^nBu_4NClO_4$) before irradiation	$E_{1/2}$/mV in MeOH (0.1 M $^nBu_4NClO_4$) after irradiation	$\tau_{1/2}$/ min	λ_{max} (ϵ, M^{-1} cm^{-1}) in MeOH/nm before irradiation	λ_{max} (ϵ, M^{-1} cm^{-1}) in MeOH/nm after irradiation
2c (H/phen)	601	573	−230	2	395(6250) 464(7750)	385(6790)[a]
2d (Me/phen)	577	552	255, −215	2	380(6700) 485(5900)	371(7570)[a]
2e (H/bpy)	585	578	270, −265	4	370(9870) 488(9970)	376(9870)[b]
2f (Me/bpy)	538	543	243, −275	5	370(7600) 480(3900)	383(8200)[b]
[Ru(*o*-C_6H_4-2-py)(phen)$_2$]PF_6	555	527				

[a] Corresponds to **2″** in Scheme 2. [b] Corresponds to **2′** in Scheme 2.

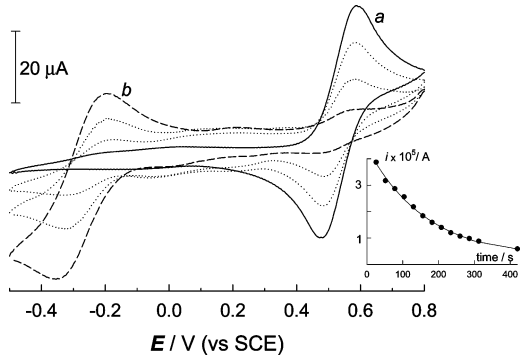

Figure 3. Cyclic voltammograms of complex **2c** (2.2 mM) in MeOH before (a, solid) and after 420 s of irradiation by a WKO ENX 360 W lamp (b, dash) obtained after subtraction of the background signal. Dotted lines illustrate changes after 104 and 208 s, respectively: 0.1 M *n*-Bu_4NClO_4, glassy carbon electrode, scan rate 0.2 V s^{-1}, 22 °C. Inset shows an exponential decay of the peak current at 0.63 V due to photosubstitution of acetonitrile ligands.

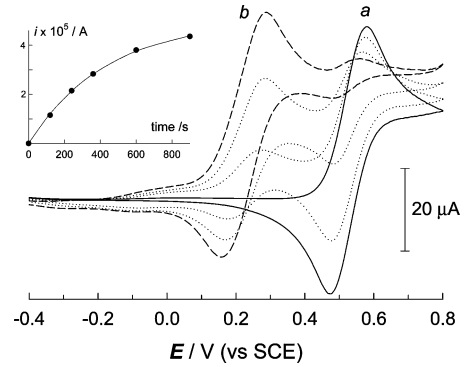

Figure 4. Cyclic voltammograms of complex **2f** (2.6 mM) in MeOH before (a, solid) and after 15 min of irradiation by a WKO ENX 360 W lamp (b, dash) obtained after subtraction of the background signal. Dotted lines illustrate changes after 2 and 6 min, respectively: 0.1 M *n*-Bu_4NClO_4, glassy carbon electrode, scan rate 0.1 V s^{-1}, 22 °C. Inset shows an exponential growth of the peak current at 0.31 V due to photosubstitution of one acetonitrile ligand.

Scheme 2. Pathways for Photochemical Solvolysis of Acetonitrile Ligands in Complexes **2**

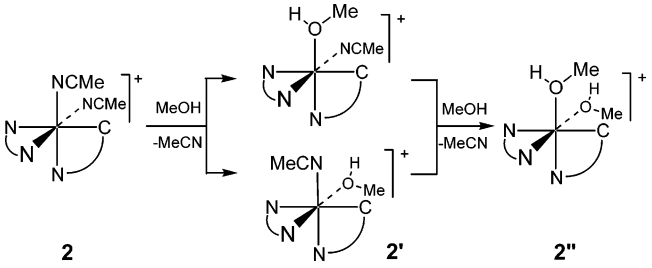

this is the first report showing that the irradiation brings about such a phenomenal lowering of redox potentials of Ru^{II} centers. More photophysical work, which is obviously beyond the scope of the present study, could reveal extra intrinsic photochemical features of the processes described in this section. Such would be useful for further applications of the effects described here in addition to the bioinorganic applications, which are reported elsewhere.[26]

Spectral Characterization of Photosolvolysis Products. Dissociation of MeCN and the oxidation into paramagnetic Ru^{III} species has been confirmed by the ^1H NMR measurements of **2c** in CD_3OD before and after its irradiation in the air for 5 min. The spectra are shown in Figure 2S of the Supporting Information. The spectrum of intact **2c** contains two resonances at δ 2.19 and 2.36 from the diastereotopic MeCN ligands. After irradiation, they collapse into a sharp singlet at δ 2.03 from liberated free CH_3CN. The signals from the cycloruthenated 2-phenylpyridine and phenanthroline ligands become broad and ill defined. This is expected because the redox potential of **2c″** equals −0.2 V, and therefore it should be oxidized into a paramagnetic Ru^{III} complex. The oxidizing agent could be either dioxygen (the evidence is presented below) or protons from traces of water as has been found in earlier studies of Ford et al.[27,28]

The formation of Ru^{III} species has been also confirmed by EPR spectroscopy. The EPR spectrum of the frozen solution used for the ^1H NMR experiment is shown in Figure 5. The *g*-factors of 1.94, 2.21, and 2.31 suggest a low-spin ($S = {}^1/_2$) octahedral monomeric Ru^{III} species. Remarkably, the spin quantitation accounts for practically all ruthenium present in the system. Note the same conclusion has been reached from the electrochemical data shown in Figure 3. The UV−vis spectrum of **2c** in MeOH has maxima at 396 (ϵ 6250) and 466 nm (ϵ 7750 M^{-1} cm^{-1}). Irradiation (in the air) brings about a noticeable fading, and the maximum shifts

(26) Ryabov, A. D.; Kurova, V. S.; Ivanova, E. V.; Le Lagadec, R.; Alexandrova, L. *Anal. Chem.*, published online Jan 20, 2005, http://dx.doi.org/10.1021/ac048743g.

(27) Hintze, R. E.; Ford, P. C. *J. Am. Chem. Soc.* **1975**, *97*, 2664−2671.
(28) Matsubara, T.; Ford, P. C. *Inorg. Chem.* **1978**, *17*, 1747−1752.

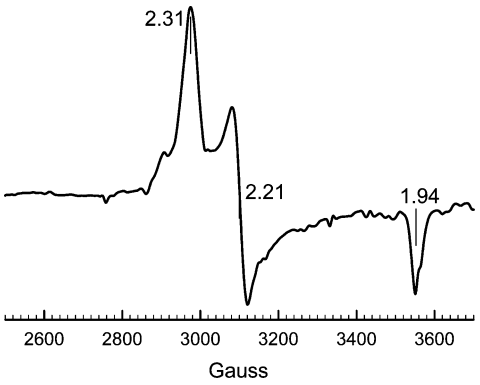

Figure 5. EPR spectrum of the frozen solution of **2c** in MeOH after irradiation for 5 min.

to 384 nm (ϵ 6790 M^{-1} cm^{-1}) in agreement with the $Ru^{II} \rightarrow Ru^{III}$ transition.[29] Other complexes **2** behave similar. The spectral characteristics are summarized in Table 1. The cycloruthenated ligand is not affected by irradiation in MeOH. This is furthermore proved by an addition of an excess of phen to the solution of **2c** after the irradiation. The solution turns gradually brownish-red. Its cyclic voltammogram indicates the formation of $[Ru(o\text{-}C_6H_4\text{-}2\text{-}py)(phen)_2]^+$ ($E_{1/2}$ = 0.555 V against 0.573 V for **2c**), which is a dominating species after 48 h and the only observed after 8 days. In addition, this result suggests simple procedures for a photochemically induced attachment of the $[Ru(o\text{-}C_6H_4\text{-}2\text{-}py)(phen)]^+$ fragment to various targets such as polymers with proper donor centers and various biomolecules including proteins, enzymes, and nucleic acid. Such an example of the interaction between the glucose oxidase enzyme and intact and photoactivated complexes of type **2** is reported elsewhere.[26]

X-ray Structural Characterization and Properties of the Oxidized Photolysis Product. It has been anticipated that irradiation of complex **2c** in methanol or acetone in the presence of chloride could open a route to low potential complexes such as *cis*-$[Ru^{III}(o\text{-}C_6H_4\text{-}2\text{-}py)Cl_2(phen)]$. We have found, however, that chloride introduces a new twist into the chemistry of these ruthenacycles. The material isolated from **2c** has a badly resolved ^1H NMR spectrum. Its IR spectrum reveals a strong band at 843 cm^{-1} due to the PF_6^- anion but does not contain signals from coordinated acetonitrile around 2265 cm^{-1} as is observed for starting complex **2c**. A structure of the isolated material has been established by the X-ray crystallography and is shown in Figure 6. The isolated compound **3** is an μ-oxo $Ru^{III}Ru^{IV}$ dimer similar to those described by Schoonover et al.[30] Particularly, cation **3** resembles the dinuclear mixed-valent species $[(bpy)_2ClRu^{III}ORu^{IV}Cl(bpy)_2](ClO_4)_3 \cdot H_2O$ (**4**). It should be mentioned that, although many μ-oxo bridged $Ru^{III}ORu^{III}$ and $Ru^{III}ORu^{IV}$ complexes have been reported

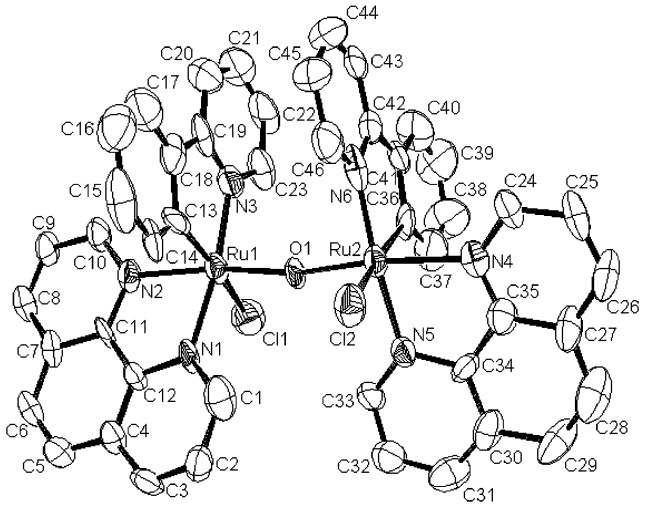

Figure 6. ORTEP diagram for the cationic part of complex **3**. Ellipsoids represent a 70% probability level. Hydrogens are omitted for clarity. Selected bond lengths: Ru1−C13 1.98(2), Ru1−N1 2.060(11), Ru1−N3 2.065(13), Ru1−N2 2.089(11), Ru1−Cl1 2.531(5), Ru2−O1 1.813(8), Ru2−N6 2.020(17), Ru2−C36 2.022(18), Ru2−N5 2.051(13), Ru2−N4 2.128(12) Å.

and studied,[31−33] complex **3** is the first structure of this type containing a cyclometalated fragment. As is shown below, the presence of the σ-bound sp^2 carbon in **3** affects noticeably some structural and electronic features of the compound.

Both Ru centers of **3** are octahedral. The chloro ligands are located in trans positions relative to the σ-bound carbon of the 2-phenylpyridine ligand. The cycloruthenated ligands are close and virtually parallel. The C(23)···C(41), C(22)···C(40), and N(3)···N(6) separations equal 3.339, 3.495, and 3.622 Å, respectively. The Ru−O bond distances in **3** equal 1.813 and 1.833 Å, and these should be compared to those of 1.805 and 1.845 Å found in complex **4**. The Ru−O−Ru bond angles equal 168.8° and 170.7° in **3** and **4**, respectively. The bond Cl−Ru−O angles are also similar in dimers **3** and **4**, (93.24°, 93.65°) and (93.6°, 95.1°), respectively. In contrast, the Ru−Cl bond distances are significantly longer in complex **3** due to the ground-state trans-effect from the σ-bound carbon, that is, 2.47 and 2.53 Å in **3** versus 2.339 and 2.357 Å in complex **4**. Consequently, the Cl···Cl separation is also higher in **3**, 6.153 versus 5.777 Å in **4** although their spatial arrangement is similar in both complexes.

Although the μ-oxo dimer **3** is to some extent an unexpected product, its formation is in general understood. A key step to μ-oxo $Ru^{III}ORu^{III}$ dimers containing N-donor ligands is the oxidation of the corresponding aqua/solvento Ru^{II} complexes by dioxygen.[31,33] Such species are generated from complexes **2** by photolysis (Scheme 3). Related μ-oxo $Ru^{III}ORu^{IV}$ dimers are usually made by electrochemical or chemical, by Ce^{IV} for example,[31] oxidation of the $Ru^{III}ORu^{III}$

(29) Ryabov, A. D.; Firsova, Y. N.; Goral, V. N.; Sukharev, V. S.; Ershov, A. Y.; Lejbolle, C.; Bjerrum, M. J.; Eliseev, A. V. *Inorg. React. Mech.* **2000**, *2*, 343−360.
(30) Schoonover, J. R.; Ni, J.-F.; Roecker, L.; White, P. S.; Meyer, T. J. *Inorg. Chem.* **1996**, *35*, 5885−5892.
(31) Weaver, T. R.; Meyer, T. J.; Adeyemi, S. A.; Brown, G. M.; Eckberg, R. P.; Hatfield, W. E.; Johnson, E. C.; Murray, R. W.; Untereker, D. *J. Am. Chem. Soc.* **1975**, *97*, 3039−3048.
(32) Gilbert, J. A.; Eggleston, D. S.; Murphy, W. R., Jr.; Geselowitz, D. A.; Gersten, S. W.; Hodgson, D. J.; Meyer, T. J. *J. Am. Chem. Soc.* **1985**, *107*, 3855−3864.
(33) Lebeau, E. L.; Adeyemi, S. A.; Meyer, T. J. *Inorg. Chem.* **1998**, *37*, 6476−6484.

Scheme 3. Proposed Mechanism for the Formation of the μ-oxo $Ru^{III}ORu^{IV}$ Dimer **3**

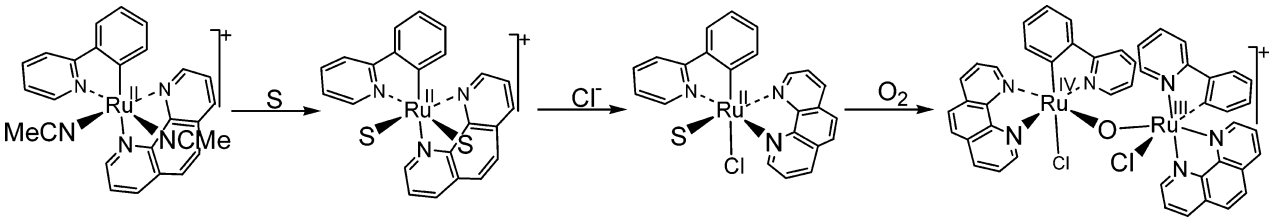

Scheme 4. Typical Oxidation States of Ruthenium in μ-oxo RuORu Dimers

$Ru^{IV}ORu^{IV}$ $\overset{+e^-}{\underset{-e^-}{\rightleftharpoons}}$ $Ru^{IV}ORu^{III}$ $\overset{+e^-}{\underset{-e^-}{\rightleftharpoons}}$ $Ru^{III}ORu^{III}$ $\overset{+e^-}{\underset{-e^-}{\rightleftharpoons}}$ $Ru^{III}ORu^{II}$

A B C

species. However, because the redox potentials of complexes **2** are substantially reduced by the presence of cycloruthenated 2-phenylpyridine as compared to bpy or phen-type ligands, the oxidation by O_2 may end up with higher oxidized, $Ru^{III}ORu^{IV}$, species. A tentative pathway to complex **3** is illustrated in Scheme 3. The coordination of chloro ligand to the product of primary solvolysis, which should involve a structural reorganization of the complex presumably via the $Ru-N_{phen}$ bond breaking or pseudo-Berry rotation within a five-coordinated species, decreases further the redox potential of the intermediate, which is then oxidized into the final product.

The fact that redox potentials of ruthenium cyclometalated complexes are significantly decreased is supported also by a cyclovoltammetric study of **3** in acetonitrile and by comparing the results with those reported for $[(bpy)_2ClRu^{III}ORu^{III}Cl(bpy)_2]^{2+}$ and **4**.[31] Complexes $[(bpy)_2ClRu^{III}ORu^{III}Cl(bpy)_2]^{2+}$ and **4** have identical voltammograms with three major reversible redox features at 1.91 (A), 0.68 (B), and -0.32 V (C) versus SSCE. Their assignment is shown in Scheme 4. The replacement of bpy by *o*-C_6H_4-2-py brings about a potential decrease by about 0.8 V with respect to each ruthenium unit. Therefore, the corresponding processes could be expected at ca. 1.1, -0.1, -1 V, respectively. In fact, we have found two well-defined quasy-reversible redox features at 0.813 and -0.221 V ($\Delta E_p \approx 100$ mV at a scan rate 0.2 V s^{-1}) in the potential range -0.5 to 1 V, which are assignable to processes A and B, respectively.

In conclusion, (1) cyclometalated ruthenium(II) 2-phenylpyridine and 2-(4-tolyl)pyridine complexes *cis*-$[Ru(o\text{-}X\text{-}2\text{-}py)(LL)(MeCN)_2]PF_6$ (**2**) with X = *o*-phenyl or *o*-4-tolyl, LL = bpy or phen, are prepared in good yields from $[Ru(o\text{-}X\text{-}2\text{-}py)(MeCN)_4]PF_6$ (**1**). (2) Both structural types, **1** and **2**, have been confirmed by X-ray crystallographic studies. (3) The complexes $[Ru(o\text{-}C_6H_4\text{-}2\text{-}py)(MeCN)_4]PF_6$ (**1a**) and $[Ru(o\text{-}MeC_6H_3\text{-}2\text{-}py)(MeCN)_4]PF_6$ (**1b**) display unusual solvent-dependent selectivity with respect to 2,2′-bipyridine and 1,10-phenanthroline. In MeCN, they react readily with phen to afford **2** but are unreactive to bpy or pyridine. (4) Irradiation of complexes **2** by visible light in methanol leads to the photochemical solvolysis of MeCN ligands. The complex *cis*-$[Ru(o\text{-}C_6H_4\text{-}2\text{-}py)(phen)(MeCN)_2]PF_6$ (**2c**) reacts most rapidly, and both MeCN ligands are substituted in a matter of 7 min. This induces an enormous, ca. 0.8 V, decrease in the redox potential from 0.57 to -0.23 V versus Ag/AgCl. (5) Attempted photochemical substitution of chloro for MeCN ligands in **2c** resulted in the unexpected formation of the crystallographically characterized μ-oxo $Ru^{III}ORu^{IV}$ dimer $[(phen)(o\text{-}C_6H_4\text{-}2\text{-}py)ClRu^{III}ORu^{IV}Cl(o\text{-}C_6H_4\text{-}2\text{-}py)(phen)]PF_6$ (**3**). Cycloruthenated complexes with either four (**1**) or two (**2**) labile acetonitrile ligands described in this work are superb building blocks for constructing a variety of different ruthenium-based assemblies, molecular wires, networks, catalysts, or simply new interesting molecules. Perspectives of using ruthenacycles in these diverse areas are currently well understood.[34−37]

Experimental Section

Methods. Mass spectra were obtained using a JEOL JMS-SX 102A instrument with *m*-nitrobenzyl alcohol as the matrix [FAB^+ mode, *m*/*z* (%, relative abundance) throughout]. Infrared spectra were recorded on a Nicolet FTIR MAGNA 750 instrument in KBr disks (ν are in cm^{-1} throughout). ^1H NMR spectra were recorded using JEOL GX 300, IBM NR/300, or Brüker Av-500 spectrometers. ^{31}P NMR spectra were recorded using a JEOL GX 300 spectrometer at 75.57 MHz. ^{13}C NMR data were obtained using JEOL GX 300 and Brüker Av-500 spectrometers at 121.65 and 125.77 MHz, respectively. The δ scale is used throughout; chemical shifts are in ppm, and the coupling constants are in Hz. ^{31}P NMR chemical shifts are versus 85% H_3PO_4. X-Band (9.62 GHz) EPR spectrum was recorded on a Bruker 300 spectrometer equipped with an Oxford ESR 910 cryostat for low-temperature measurements.[38] Cyclic voltammetry measurements were performed using a EG& G Princeton Applied Research potentiostat/galvanostat model 270/250 or Autolab potentiostat/galvanostat under N_2 using glassy carbon as working electrode, Pt wire as a counter electrode, and SCE or Ag/AgCl as reference electrodes. Unless otherwise stated, all potentials indicated in the text are versus Ag/AgCl. The working electrode was always polished with a diamond paste (Struers) before each measurement. Solutions of the photolabile acetonitrile Ru^{II} complexes were irradiated with a WKO ENX 360 W lamp conventionally used as a light source in overhead projectors. It was placed 10−15 cm from the irradiated solution. A potential of 45−50 V generated by a Fischer transformer was applied. During the experiments, the lamp was cooled by a stream of air using either a heat gun or an air line. Microanalyses have been performed at the Service de microanalyses of the Institut de Chimie at Strasbourg

Materials. Ligands 2-phenylpyridine and 2-(4-tolyl)pyridine were purchased from Aldrich and used as received. All other

(34) Bonnefous, C.; Chouai, A.; Thummel, R. P. *Inorg. Chem.* **2001**, *40*, 5851−5859.
(35) Hadadzadeh, H.; DeRosa, M. C.; Yap, G. P. A.; Rezvani, A. R.; Crutchley, R. J. *Inorg. Chem.* **2002**, *41*, 6521−6526.
(36) Hortholary, C.; Minc, F.; Coudret, C.; Bonvoisin, J.; Launay, J.-P. *J. Chem. Soc., Chem. Commun.* **2002**, 1932−1933.
(37) Fraysse, S.; Coudret, C.; Launay, J.-P. *J. Am. Chem. Soc.* **2003**, *125*, 5880−5888.
(38) Petasis, D. T.; Hendrich, M. P. *J. Magn. Reson.* **1999**, *136*, 200−206.

Scheme 5. Numbering Scheme Used for the Chemical Shift Assignment[a]

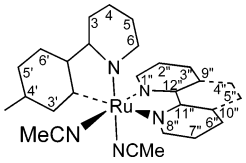

[a] 9″−12″ are tertiary carbons.

chemicals used in this work were commercially available materials usually purchased from Aldrich except $RuCl_3 \cdot nH_2O$, which was a Strem reagent. Starting complexes **1a**,**b** were made by cycloruthenation of the corresponding amines by $[(\eta^6\text{-}C_6H_6)RuCl(\mu\text{-}Cl)]_2$ as originally described for **1a**.[16] The Ru complex (1.5 g, 3.01 mmol), KPF_6 (2.22 g, 12.04 mmol), NaOH (0.48 g, 6.02 mmol), and arylpyridine (6.02 mmol) were stirred in 50 mL of MeCN at 45−50 °C for 20 h. The resulting yellow slurry was evaporated to dryness under reduced pressure, and the residue was purified by column chromatography on Al_2O_3 (preferably Alumina 90 from Merck) using CH_2Cl_2 or MeCN as eluents. The yellow band was collected and evaporated to dryness. Bright yellow crystals used for X-ray analysis were obtained by a slow diffusion of diethyl ether into a concentrated solution of the yellow solid in a mixture of CH_2Cl_2:MeCN (1:1 v/v). Complex **1a** (68%): ^{1}H NMR (d_3-MeCN, see Scheme 5 for the numbering) 8.89 (d, 1H, ^3J 6.0, H6), 7.95 (dd, 1H, ^3J 7.4, ^4J 0.8, H3′), 7.86 (d, 1H, ^3J 8.2, H3), 7.72 (td, 1H, ^3J 8.0, ^4J 1.5, H4), 7.70 (d, 1H, ^3J 6.0, H6′), 7.15 (td, 1H, ^3J 6.0, ^4J 1.4, H5), 7.07 (td, 1H, ^3J 7.4, ^4J 1.4, H4′), 6.95 (td, 1H, ^3J 7.7, ^4J 0.8, H5′), 2.49 (s, 3H, $NCCH_3$), 2.13 (s, 3H, $NCCH_3$), 1.94 (s, 6H, $NCCH_3$). ^{13}C NMR: 184.27, 168.20, 152.47, 146.87, 138.31, 136.11, 127.59, 123.23, 121.21, 120.65, 117.77, 3.44, 2.89. ^{31}P NMR: 143 (sept, PF_6). IR: 834 (s, PF_6), 2268 (m, MeCN). MS: 419(5%) $[M + H]^+$, 379(63) $[(M + H) - MeCN]^+$, 338(37) $[(M + H) - 2MeCN]^+$, 297(45) $[(M + H) - 3MeCN]^+$, 256(36) $[(M + H) - 4MeCN]^+$. Complex **1b** (63%). Anal. Calcd for $C_{20}H_{22}F_6N_5PRu \cdot {}^1/_3\{(C_2H_5)_2O\}$: C, 42.48; H, 4.23; N, 11.61. Found: C, 42.24; H, 4.17; N, 11.16. ^{1}H NMR (d_3-MeCN): 8.86 (dd, 1H, ^3J 6.0, ^4J 0.8, H6), 7.76 (d, 1H, ^3J 8.0, H3), 7.72 (s, 1H, H3′), 7.70 (td, 1H, ^3J 8.0, ^4J 1.4, H4), 7.60 (d, 1H, ^3J 7.7, H6′), 7.10 (td, 1H, ^3J 7.2, ^4J 1.4, H5), 6.76 (d, 1H, ^3J 7.7, H5′), 2.51 (s, 3H, CH_3), 2.35 (s, 3H, $NCCH_3$), 1.99 (s, 6H, $2NCCH_3$), 1.95 (s, 3H, $NCCH_3$). ^{31}P NMR: 144 (sept, PF_6). IR: 839 (s, PF_6), 2250 (m, $NCCH_3$). MS: 434(4%) $[M + H]^+$, 393(30%) $[(M + H) - MeCN]^+$, 352(10%) $[(M + H) - 2MeCN]^+$, 311(15%) $[(M + H) - 3MeCN]^+$, 270-(7%) $[(M + H) - 4MeCN]^+$.

Synthesis of 2c. Complex **1a** (0.33 g, 0.585 mmol) and phen (0.105 g, 0.583 mmol) were degassed in a vacuum, the flask was purged three times with N_2, and dry MeCN (40 mL) was added. The mixture was stirred at room temperature under N_2 for 15 h. Solvent was evaporated; the residue was dissolved in 10 mL of CH_2Cl_2 and brought on a column with basic Al_2O_3. The first band eluted with $CHCl_3$ was concentrated, poured into Et_2O, and kept at −5 °C. Brownish-red crystals of **2c** (0.32 g, 83%) were air-dried and used for the X-ray study. Anal. Calcd for $C_{27}H_{22}F_6N_5PRu$: C, 48.9; H, 3.4; N, 10.6. Found: C, 48.9; H, 3.7; N, 10.0. IR: 841 (vs, PF_6), 2265 (m, MeCN). ^{1}H NMR (d_3-MeCN): 9.70 (dd, 1H, ^3J 5.0, ^4J 1.4, H8″), 8.71 (dd, 1H, ^3J 8.2, ^4J 1.4, H3), 8.28 (dd, 1H, ^3J 7.5, ^4J 1.3, H3′), 8.22−8.13 (m, 3H), 8.16 (d, 1H, ^3J 9.0, H4″ or H5″), 8.02 (d, 1H, ^3J 9.0, H4″ or H5″), 7.85 (td, 2H, ^3J 7.5, ^4J 0.8, H4′), 7.46 (td, 1H, ^3J 7.4, ^4J 1.5, H7″), 7.36−7.32 (m, 2H), 7.27 (dd, 1H, ^3J 7.2, ^4J 1.1, H4), 7.10 (td, 1H, ^3J 7.7, ^4J 1.1, H5′), 6.57 (td, 1H, ^3J 7.2, ^4J 1.3, H5), 2.28 (s, 3H, $NCCH_3$), 2.06 (s, 3H, $NCCH_3$) 9.70. ^{31}P NMR (CD_3CN): 141 (sept, PF_6). MS: 518 (4%) $[M + H]^+$, 477(4%) $[(M + H) - MeCN]^+$, 436-(5%) $[(M + H) - 2MeCN]^+$.

Synthesis of 2d. Complex **1b** (0.50 g, 0. 0.865 mmol) and 1,10-phenanthroline (0.143 g, 0.796 mmol) were stirred in 30 mL of acetonitrile at room temperature for 20 h. The resulting deep purple solution was evaporated to dryness under reduced pressure, and the residue was purified by column chromatography on Al_2O_3 using CH_2Cl_2:MeCN (5:1 v/v) as an eluent. The purple band was collected and evaporated to dryness. Dark brownish-purple crystals were obtained by a slow diffusion of diethyl ether into a concentrated solution of **2e** in a CH_2Cl_2:MeCN mixture (5:1 v/v). Yield 0.49 g (70%). MS: 677(3%) $[(M + H) + PF_6]^+$, 532(10) $[M + H]^+$, 491(30) $[(M + H) - MeCN]^+$, 450(30) $[(M + H) - 2MeCN]^+$, 250(20) $[(M + H) - 2MeCN - phen]^+$. IR (KBr): 836 (s, PF_6), 2264 (m, MeCN). ^{1}H NMR (d_3-MeCN): 9.69 (dd, 1H, ^3J 5.0, ^4J 1.4, H8″), 8.70 (dd, 1H, ^3J 8.2, ^4J 1.4, H3), 8.20−8.14 (m, 4H), 8.08 (s, 1H, H3′), 8.00 (d, 1H, ^3J 9.0, H4″ or H5″), 7.78−7.73 (m, 2H), 7.45−7.28 (m, 3H), 6.90 (dd, 1H, ^3J 7.9, ^4J 1.9, H5′), 6.52 (td, 1H, ^3J 5.8, ^4J 1.4, H5), 2.48 (s, 3H, CH_3), 2.27 (s, 3H, $NCCH_3$), 2.14 (s, 3H, $NCCH_3$). ^{31}P NMR (CD_3CN): 144 (septet, PF_6). Anal. Calcd for $C_{26}H_{24}F_6N_5PRu$: C, 49.71; H, 3.58; N, 10.35. Found: C, 49.76; H, 3.66; N, 10.31.

Synthesis of 2e and 2f. A solution of complex **1a** or **1b** (0.865 mmol) and 2,2′-bipyridine (143 mg, 0.796 mmol) in 30 mL of CH_2Cl_2 was stirred at room temperature for 20 h. The resulting deep purple solution was evaporated to dryness under reduced pressure, and the residue was purified by column chromatography on Al_2O_3 using CH_2Cl_2 as an eluent. The purple band was collected and evaporated to dryness. Dark purple crystals were obtained by a slow diffusion of diethyl ether into a concentrated solution of the purple solid in a CH_2Cl_2:MeCN mixture (1:1 v/v). **2e**. Yield 0.41 g (74%). MS (FAB^+): 494(4%) $[M + H]^+$, 453(5) $[(M + H) - MeCN]^+$, 412(5) $[(M + H) - 2MeCN]^+$. IR (KBr): 839 (s, PF_6), 2245 (m, MeCN). ^{1}H NMR (d_3-MeCN): 9.35 (dd, 1H, ^3J 6.0, ^4J 0.8, H8″), 8.44 (d, 1H, ^3J 7.9, H3′), 8.20 (m, 2H), 7.90−7.75 (m, 4H), 7.65 (td, 1H, ^3J 7.5, ^4J 0.8, H6″), 7.50 (td, 1H, ^3J 7.5, ^4J 0.8, H3"), 7.43 (dd, 1H, ^3J 6.0, H1″), 7.28−7.14 (m, 2H), 7.08−6.98 (m, 2H), 6.72 (td, 1H, ^3J 5.8, ^4J 1.4, H5), 2.21 (s, 3H, $NCCH_3$), 2.14 (s, 3H, $NCCH_3$). ^{31}P NMR (CD_3CN): 150 (septet, PF_6). Anal. Calcd for $C_{25}H_{22}F_6N_5PRu$: C, 47.03; H, 3.47; N, 10.97. Found: C, 47.26; H, 3.74; N, 10.79. **2f**. Yield: 0.49 g (71%). MS (FAB^+): 653-(29%) $[(M + H) + PF_6]^+$, 508(28) $[M + H]^+$, 467(30) $[(M + H) - MeCN]^+$, 426(98) $[(M + H) - 2MeCN]^+$, 270(20) $[(M + H - 2MeCN - bpy)]^+$. IR: 842 (s, PF_6), 2259 (m, MeCN). ^{1}H NMR (d_3-MeCN): 9.34 (dd, 1H, ^3J 6.0, ^4J 0.8, H8″), 8.43 (dd, 1H, ^3J 7.1, ^4J 0.8, H3′), 8.22−8.15 (m, 2H), 8.01 (s, 1H, H3′), 7.89−7.65 (m, 5H), 7.48 (td, 1H, ^3J 8.0, ^4J 0.8, H6″), 7.39 (dd, 1H, ^3J 6.0, ^4J 0.8, H1″), 6.99 (td, 1H, ^3J 5.9, ^4J 1.4, H3″), 6.87 (dd, 1H, ^3J 7.7, ^4J 0.8, H6′), 6.67 (td, 1H, ^3J 5.9, ^4J 1.4, H5), 2.45 (s, 3H, CH_3), 2.20 (s, 3H, $NCCH_3$), 2.19 (s, 3H, $NCCH_3$). ^{31}P NMR: 136 (septet, PF_6). Anal. Calcd for $C_{26}H_{24}F_6N_5PRu$: C, 47.86; H, 3.71; N, 10.73. Found: C, 47.68; H, 3.72; N, 10.62.

Synthesis of 3. A: Complex **2c** (0.05 g, 0.075 mmol) was dissolved in acetone (13 mL) in the presence of Et_4NPF_6 (0.03 g, 0.11 mmol) and $Et_4NCl \cdot H_2O$ (0.04 g, 0.22 mmol). The mixture was irradiated with the WKO ENX 360 W lamp as described above for 50 min. The reaction progress was controlled by TLC. The solution volume was then reduced to 4 mL, and the precipitate formed was filtered off, washed rapidly with cold water, and dried in a vacuum. Anal. Calcd for $C_{46}H_{32}Cl_2F_6N_6OPRu_2 \cdot 8H_2O$: C, 44.3; H, 3.9; N, 6.7. Found: C, 44.3; H, 4.8; N, 6.5. B: Complex **1a** (0.065 mmol) was refluxed for 60 min in 11.25 mL of MeOH with 0.065 mmol of phen. An excess of LiCl was added, and the mixture

Table 2. Crystallographic Data and Summary of Data Collection and Structure Refinement

	1a	1b	2d	3
formula	$C_{23}H_{30}F_6N_5OPRu$	$C_{22}H_{27}F_6N_5O_{1/2}PRu$	$C_{28}H_{24}F_6N_5PRu$	$C_{46}H_{32}Cl_2F_6N_6OPRu_2$
fw	638.56	615.53	676.56	1102.811
diffractometer	Bruker Smart Apex CCD	Bruker Smart Apex CCD	Bruker Smart Apex CCD	Bruker Nonius KappaCCD
wavelength, Å	0.71073	0.71073	0.71073	0.71073
crystal system	triclinic	triclinic	monoclinic	triclinic
space group	$P\bar{1}$	$P\bar{1}$	$P2_1/n$	$P\bar{1}$
T, K	293(2)	291(2)	293(2)	223
a, Å	8.622(1)	8.5645(5)	15.195(2)	11.531(1)
b, Å	8.625(1)	8.7292(5)	12.169(2)	12.262(1)
c, Å	20.225(1)	18.5882(11)	16.855(2)	17.186(2)
α, deg	80.007(2)	97.1170(10)	90.00	93.533(4)
β, deg	78.965(2)	95.4670(10)	113.263(3)	94.226(4)
γ, deg	81.777(2)	98.5230(10)	90.00	103.916(4)
V, Å^3	1444.4(2)	1354.57(14)	2863.2(7)	2344.4(4)
Z	2	2	4	2
D_{calc}, g cm^{-3}	1.468	1.509	1.569	1.562
θ range (deg) for data collection	2.08−25.00	2.22−32.69	1.53−32.63	4.076−25.682
$N_{measured}$	17 139	11 218	38 385	15 064
$N_{independent}$	5102	4785	10 396	4807
R	0.0683	0.0599	0.0690	0.0897
wR_2	0.1525	0.1466	0.0832	0.206
GOF	1.072	1.027	0.942	1.149
largest diff between peak and hole (e Å^{-3})	1.045 and −0.453	1.061 and −0.488	0.520/−0.533	1.07/−0.55
cryst size, mm^3	0.040 × 0.276 × 0.366	0.39 × 0.19 × 0.07	0.038 × 0.124 × 0.224	0.1 × 0.1 × 0.2

was refluxed for ca. 5 h. The mixture was separated by TLC chromatography on Al_2O_3. Complexes **2c** and **3** were isolated (the latter gave a positive reaction on chloride with $AgNO_3$). The crystals of **3** were obtained as follows. A solution of **3** (4 mg in 1 mL of $CHCl_3$) was placed in a NMR tube with a cotton cork. *n*-Hexane (2 mL) was slowly dribbled to form two discreet layers. A slow diffusion of hexane into chloroform and evaporation of the solvents gave crystals of **3** used for the X-ray investigation.

X-ray Structure Determination. Crystal data, data collection, and refinement parameters are given in Table 2. Diffraction intensity data were collected with diffractometers equipped with a graphite-monochromated Mo Kα radiation source. The data collected were processed to produce conventional intensity data by the program SAINT-plus.[39] The intensity data were corrected for Lorentz and polarization effects. Absorption correction was applied using the face-indexed method. The structures were solved by direct methods and completed by subsequent difference Fourier syntheses and refined by full matrix least-squares procedures on F^2. All non-hydrogen atoms were refined anisotropically. Hydrogen atom positions were calculated and included in the final cycle of refinement. Highly disordered PF_6 anions in some cases were modeled into two major contributors with only the common atoms refined anisotropically. All calculations were performed by the SHELXTL (6.10) program package.[40]

Acknowledgment. L.A. and R.L.L. thank CONACyT (34293-E and 40135-Q) for support. Assistance from Caleb Curver in recording ESR spectra and M. S. Miguel Canseco in obtaining UV−vis data is gratefully acknowledged.

Supporting Information Available: X-ray crystallographic data (CIF); X-ray data for **2c**; ^{1}H NMR spectra of intact and irradiated **2c**. This material is available free of charge via the Internet at http://pubs.acs.org.

IC048270W

(39) *Bruker SMART (Version 5.625), SAINT-Plus (Version 6.23C)*; Bruker AXS Inc.: Madison, WI, 1999.

(40) Sheldrick, G. M. *SHELXTL (Version 6.10)*; Bruker AXS Inc.: Madison, WI, 2000.